IEEE Photonics Journal
An IEEE Photonics Society Publication

Open Access

Coherent Perfect Absorber Based on Antisymmetric Metasurface With Gain Material

Volume 12, Number 3, June 2020

Ming Chen
Chen Chen
Shijie Deng
Chongyun Wang
Houquan Liu
Chuanxin Teng
Yu Cheng
Hongyan Yang
Ronghui Xu
Hongchang Deng
Libo Yuan

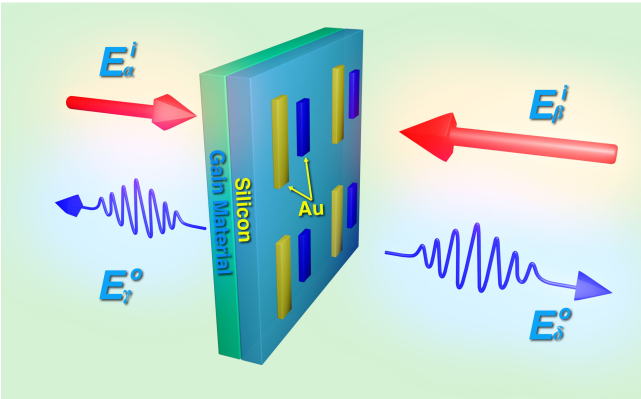

DOI: 10.1109/JPHOT.2020.2992100

IEEE photonics SOCIETY
IEEE

Coherent Perfect Absorber Based on Antisymmetric Metasurface With Gain Material

Ming Chen,[1] Chen Chen,[2] Shijie Deng,[1] Chongyun Wang,[2] Houquan Liu,[1] Chuanxin Teng,[1] Yu Cheng,[1] Hongyan Yang,[1] Ronghui Xu,[1] Hongchang Deng,[1] and Libo Yuan[1]

[1]Photonics Research Centre, School of Electronic Engineering and Automation, Guilin University of Electronics Technology, Guilin 541004, China
[2]School of Information and Communication, Guilin University of Electronics Technology, Guilin 541004, China

DOI:10.1109/JPHOT.2020.2992100

Manuscript received February 2, 2020; revised April 19, 2020; accepted April 29, 2020. Date of publication May 4, 2020; date of current version May 26, 2020. This work was supported in part by he National Key Research and Development Program of China under Grant 2019YFB2203903, in part by the National Natural Science Foundations of China under Grants 61965006, 61975038, 6194005, and 61640409, in part by the Natural Science Foundation of Guangxi Province under Grants 2017GXNSFAA198048, 2018GXNSFAA294099, and 2019GXNSFBA245057, in part by Guangxi Project under Grant AD18281092, and in part by the foundation from Guangxi Key Laboratory of Automatic Detecting Technology and Instruments under Grant YQ20107. M.Chen and C.Chen contributed equally to this work. Corresponding author: Yu Cheng (e-mail: chengyu@guet.edu.cn).

Abstract: In this paper, we proposed a two ports coherent perfect absorber based on antisymmetric metasurface with gain material which is able to effectively regulate the absorption of the coherent incident wave under the condition of unequal incident intensities. This design overcomes the limitation that exists in the previous coherent controller which can only be applied to coherent light of equal intensity without gain material. In the proposed absorber, the metal strips of different lengths are arranged in an antisymmetric manner on the interlayer, a gain material layer is introduced to regulate the unequal intensity coherent light and the electromagnetic response mode which can be selectively strengthened and weakened by modulating the phase difference between two incident waves, and a high coherent absorption under the condition of asymmetric incident wave can be realized. Results show that the proposed absorber achieve coherent perfect absorption at the frequency of 15.25 THz and 17.75 THz, which can change the total absorption in the range from 27.41% to 98.55%, and from 27.55% to 97.88%, respectively. This paper may serve as an important tool for all-optical information transmission and data processing.

Index Terms: Absorber, metasurface, gain material.

1. Introduction

With the development of optical fiber communication [1], the disadvantages of electronic devices such as power consumption and low efficiency are gradually exposed, resulting in the phenomenon of electronic bottleneck in communication network [2]. In order to solve this problem, all-optical communication technology [3] has attracted a lot of attentions recently. All-optical data processing devices are of great importance to the development of all-optical communication networks, but there is no optical transistor available that provides similar performance to the electronic transistor.

Researchers have spent a lot of effort trying to develop high-efficiency nonlinear media to improve the performance of optical transistors [4].

However, according to Huygens' principle of wave superposition, when light waves propagates into a linear medium, it will propagate independently in its own direction and will not interact with other light waves [5]. In the framework of classical electrodynamics, this superposition principle for electromagnetic waves in vacuum or interacting internally has not been challenged [6], [7] and researchers have used a strong laser field to promote the beam interaction in nonlinear media.

To overcome this difficulties, coherent control technology provides a new method to control the interaction between optical materials and electromagnetic fields. As a new technology, coherent control technology has aroused a great interest of researchers. Coherent control of polarization and refraction effects by using these structures can also be realized [8]–[10]. In 2012, Zhang et al. demonstrated that any two coherent beams of low intensity can interact on nanoscale thick metamaterials, causing one beam to modulate the intensity of the other beam, and when the intensities of the two beams are equal, all light entering the metamaterial will be absorbed [11]. In 2018, Papaioannou et al. demonstrate that the dynamic control of focus can be achieved by coherent interaction of the beam on the plasma metasurface which was manufactured by thermal evaporation of gold layer on a silicon nitride membrane, subsequent silicon nitride removal by reactive ion etching to build a gold film splitter, can be turned on and off by changing the control pattern, phase, or intensity. [12]. In recent work, researchers have experimentally demonstrated that the terahertz bandwidth photoelectric modulation process can be carried out on metamaterials to achieve the process of coherent absorption (in principle, this coherent absorption is only affected by the spectral width of metamaterial absorption resonance) [13]–[15]. They experimentally verified that ultra-thin plasma metamaterials can achieve coherent perfect absorption (CPA) and coherent perfect transmission (CPT) respectively [16]–[18]. Zhu et al. [19] designed an ultra-thin metasurface consisting of a single-layer all-dielectric structure, and demonstrated that CPA can be achieved in all-dielectric metasurface in 2016. Metasurface has produced many unconventional optical properties as well as novel physical phenomena and applications [20], [21]. In the field of all-optical data processing, the difficulties exist to effectively regulate the total absorption rate of incident waves under asymmetric incident conditions. The emergence of all-optical information processing can be more energy saving, more environmental protection. CPA is achieved by the interference of two incident beams from both sides of the sample. Initially, CPA was studied by modulating the absorption of a thick silicon plate as the phase difference between two beams with equal intensities changed, not by a gain material.

In this paper, we propose an absorber based on metasurface with gain material that allow the regulation of the absorption rate of a strong signal beam by using a weaker control beam. This design is composed of rectangular metal strips of different lengths carried by two layers of silicon and gain medium and antisymmetric which on both sides. Coherent absorption can be achieved by reasonably setting the structural parameters, adjusting the surface conductivity and substrate refractive index. The loss of incident light can be adjusted in the proposed device by introducing a gain material. The phase difference between two coherent waves is changed to control the absorption rate, which provides a new idea for absorption modulation. By adjusting the phase difference between the incident waves, the coherent proposed absorber can achieve coherent perfect absorption at the frequency of 15.25 THz and 17.75 THz and changing in the range from 27.41% to 98.55%, and from 27.55% to 97.88%, respectively.

2. Theoretical Analysis

A coherent controller is a type of functional device that can control coherent electromagnetic waves in multiple modes, and can be used as an optical switch or amplifier [22] which usually has two ports. The mechanism for achieving CPA is described as follows: two coherent light waves propagate in opposite directions and are vertically incident on the metasurface. Adjusting the phase difference between the two coherent waves, the position of the standing wave in the metasurface can be changed and the absorption can be varied [23].

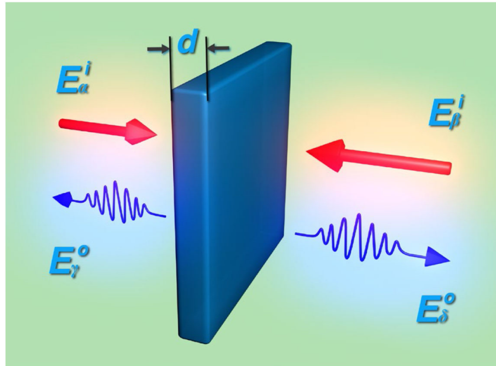

Fig. 1. Schematic of a dual-port coherent controller with two counterpropagating input waves (E_α^i and E_β^i), E_γ^o and E_δ^o representing the output waves.

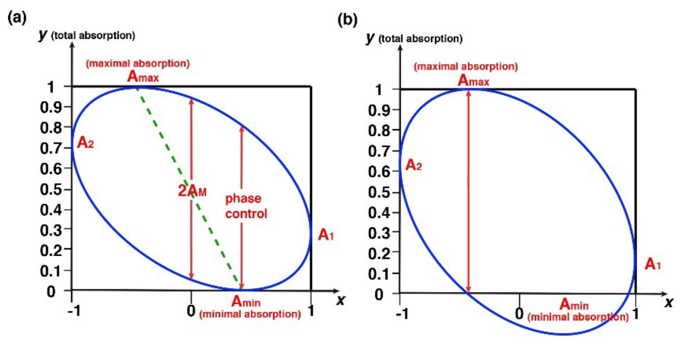

Fig. 2. (a) A dual-port optical system scattering matrix diagram using only lossy materials without gain material; (b) a dual-port optical system scattering matrix diagram that may be obtained by combining the lossy material and the gain material.

CPA is related to the analytic properties of the scattering matrix (S matrix). For simplicity, we consider the scattering in two dimensions. In the case of symmetrical and reciprocity, the complex scattering coefficients of output waves (E_γ^o and E_δ^o) can be written as [24]:

$$\begin{bmatrix} E_\gamma^o \\ E_\delta^o \end{bmatrix} = S \begin{bmatrix} E_\alpha^i \\ E_\beta^i \end{bmatrix} = \begin{bmatrix} t & r \\ r & t \end{bmatrix} \begin{bmatrix} E_\alpha^i \\ E_\beta^i \end{bmatrix} \tag{1}$$

where E_α^i and E_β^i representing the input coherent waves from the opposite sides, E_γ^o and E_δ^o are the output waves. r and t are the reflection and transmission coefficients respectively, whose expression is given by

$$r = \frac{\left(n^2 - 1\right)\left(-1 + e^{i2nkd}\right)}{(n+1)^2 - (n-1)^2 e^{i2nkd}} \tag{2}$$

$$t = \frac{4ne^{inkd}}{(n+1)^2 - (n-1)^2 e^{i2nkd}} \tag{3}$$

Here, n is the refractive index, k $=\omega/c$ is wave vector, and d is the thickness of the metasurface. From Equations. (2) and (3), the conditions for normal production of CPA can be described as:

$$\exp\left(inkd\right) = \pm\frac{n-1}{n+1} \tag{4}$$

In Fig. 2, A_1 and A_2 are the single-beam absorption, i.e., the absorbance observed when the system is excited by either side 1 or side 2, and x is the imbalance factor accounting for the power difference between the two waves input intensities:

$$x = \left(\left|E_\alpha^i\right|^2 - \left|E_\beta^i\right|^2\right) / \left(\left|E_\alpha^i\right|^2 + \left|E_\beta^i\right|^2\right) \tag{5}$$

And the ellipse which is shown in Fig. 2 can be described as [25]

$$A = 1 - \frac{\left|E^o\right|}{\left|E^i\right|} = \frac{1+x}{2}A_1 + \frac{1-x}{2}A_2 - \sqrt{1-x^2}A_M \sin(\phi + \delta) \tag{6}$$

Here,

$$A_M = \sqrt{(1-A_1)(1-A_2) - \left|\det S\right|^2} \tag{7}$$

which represents the depth of the phase modulation. When the system is driven from a single port, i.e., $x = \pm 1$, the absorption become the ordinary single-beam absorption $A_{1,2} = 1-|r|^2-|t|^2$ which can be controlled by the relative phase $\phi = \arg(E_\beta^i / E_\alpha^i)$ of two input waves and δ is the device phase. The CPA phenomenon corresponds to the zero point of the scattering matrix ($E_\gamma^o = E_\delta^o = 0$).

Fig. 2(a) shows the S matrix diagram which is obtained by designing a dual-port optical system consisting of only lossy materials. When the incident wave intensities of the two ports are not equal (the abscissa value is not 1), by controlling the phase shift from 0 to π, CPT can be achieved. However, this method is not able to make the ordinate value negative as it is dependent on energy conservation. As a result, the device can't achieve the CPA by simple phase modulation. As shown in Fig. 2(b), for devices are fabricated with lossy materials and gain materials, the ellipse can exhibit a negative value which means the output power is greater than the input power and the absorption can be regulated when the control wave intensity is not equal at the same time [26].

3. Design Description

In the proposed absorber, the total absorption rate is regulated effectively under the condition of unequal incident intensity by introducing a gain material combined with a common lossy material. This overcomes the exiting limits incoherent control devices which can only be used to regulate equal-intensity coherent light. The absorber consists of parallel metal film materials with different lengths, which are anti-symmetrically arranged on both sides of the substrate in a periodic array, as shown in Fig. 3. "A" and "B" represent two metal strips of different lengths. The thickness of metal strips is $t = 30$ nm, the width of metal strips are $W_A = W_B = 0.8$ μm, and the length are $L_A = 2.5$ μm and $L_B = 2$ μm, respectively; the thickness of the silicon substrate is $H_1 = 0.15$ μm, and the thickness of the gain material substrate is $H_2 = 0.15$ μm; the unit period is $P = 3$ μm. In the simulation, we introduce optical gain through the imaginary part of the complex dielectric constant, and the dielectric constant of the gain material is $4.05 + 0.05i$. The schematic diagrams of the "on" and "off" state of the device are shown in Fig. 3(b) and 3(c). It can be seen that, in the "on" state, the input wave and the control wave will completely transmit through the device; in the "off" state, the input wave and the control wave will be completely absorbed.

The proposed absorber was modeled and simulated by using COMSOL Multiphysics. Periodic boundary conditions are applied in the x and y directions; the distance between the absorber and the two ports in the z direction is 5μm. From these two ports, a pair of coherent waves with power of 1W and 0.2W are set opposite. The phase difference of the coherent light signal is set to 0 initially. A perfect matching layer of 3μm thick is added to the outer side of the two ports to prevent additional reflection. Planes are intercepted on each of the two sides, and the surface integral of the average power on both planes can be used to calculate the total output power. With the required parameters, simulation is performed in the frequency domain range of 12 THz to 20 THz.

4. Numerical Analysis

When the structural parameters are fixed and the wave with a certain power, the total output power P_{out} of two ports can be obtained by surface integration of the time-average power flow at the cross

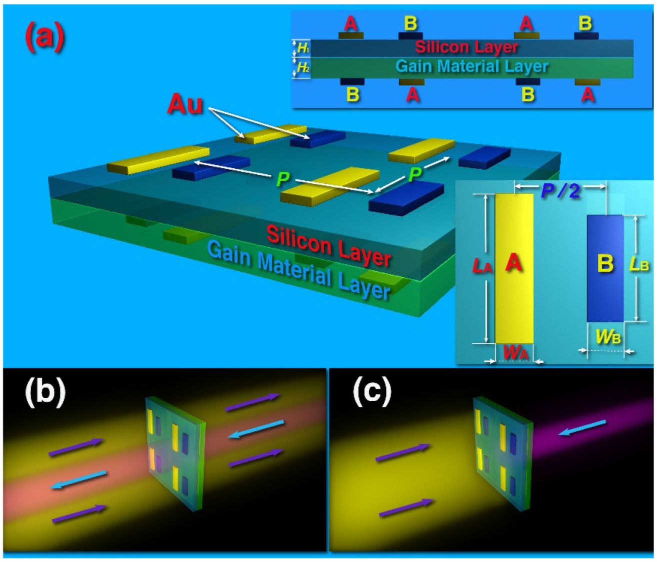

Fig. 3. (a) The schematic diagram of absorber and the side view (upper right corner) of designed coherent control metamaterial structure, and the top view of one structural unit (bottom right corner); P is the unit structure period; H_1 and H_2 are the thickness of the silicon substrate and the gain material substrate, respective; L_A and L_B are the length of "A" and "B", W_A and W_B are the width of "A" and "B", respective; (b)The schematic diagram of the "on" and (c) "off" state of the designed device.

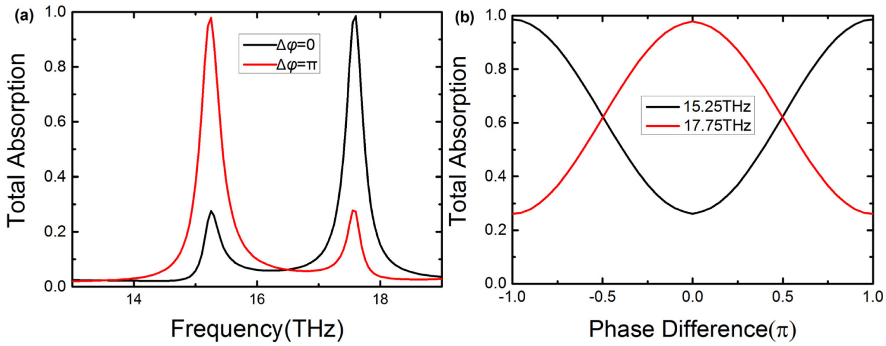

Fig. 4. (a) The absorption rate of proposed absorber when the phase difference between the coherent incident waves is 0 and π. (b)The total absorption rate as a function of phase difference at the frequency of 15.25 THz and 17.75 THz.

section of two ports, The total absorption rate of the proposed device can be calculated as follows:

$$A_{\text{total}} = 1 - P_{\text{out}}/P_{\text{in}} \quad (8)$$

It can be seen from Fig. 4(a) that the total absorption rate is 98.55% at 17.75 THz when the phase difference between the coherent incident wave $\Delta\varphi$ is 0. The P_{out} reaches the lowest value of only 0.017 W when P_{in} and the power of the control wave is 0.2 W. While the total absorption rate is 97.88% at 15.25 THz when $\Delta\varphi$ is π, which can be regarded as approximately perfect absorption. In our experiment, the modulation depth of the proposed device is about 5.6 dB and the modulation bandwidth is 0.296 THz which is larger than EAM (electroabsorption modulator).

In order to facilitate the discussion of the phase modulation performance of the coherent absorber, we control the phase of the lower power incident wave so that the phase difference between the two input coherent incident waves can be changed. The phase difference between the incident waves $\Delta\varphi$ is varied with a step of 0.1π increasing from -π to π, with fixed structural parameters. The absorption rate at different phase differences is calculated with the resonant

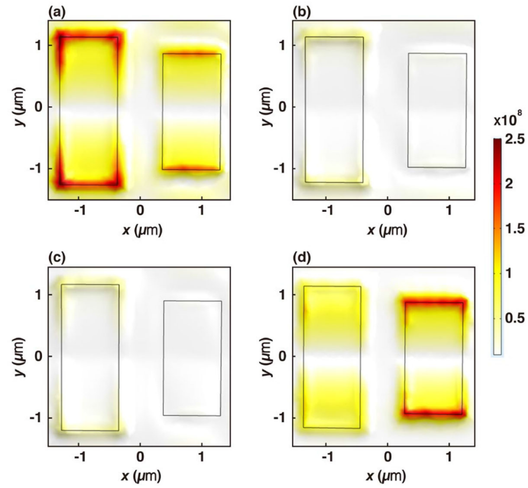

Fig. 5. The electric field distribution of when the phase difference between the coherent incident waves is 0 and π at (a)(b)15.2THz and (c)(d)17.75THz.

frequency of 17.75 THz and 15.25 THz (the phase difference between the coherent waves is 0 and π, respectively). It can be seen from Fig. 4(b) that the absorber has the highest total absorption rate for coherent incident waves, reaching 98.55% at frequency of 17.75 THz when $\Delta\varphi$ is 0, and 97.88% at frequency of 15.25 THz when $\Delta\varphi$ is π. When the absolute value of the phase difference is increased, the total absorption rate of the coherent incident wave gradually decreased and the total absorption rate reaches the lowest value of 27.41% at a phase difference of $\pm\pi$. This indicates that the designed coherent perfect absorber can be arbitrarily adjusted between 27.41% and 98.55% at 17.75 THz under asymmetric incidence conditions by adjusting the phase difference between the incident waves. Conversely, at the frequency of 15.25 THz, the absorption rate can be increased from 27.55% to 97.88% by adjusting the phase difference from 0 to π. Therefore, the proposed coherent perfect absorber realizes the manipulation of the absorption rate of the high intensity wave by the low power wave which is the control wave.

To further analyze the mechanism of the CPA phenomenon and the perfect coherent control device, the electric field distribution on the absorber in the simulation is monitored. Fig. 5(a) and 5(b) shows the electric field intensity distribution at the resonant frequency when the phase difference $\Delta\varphi$ between the incident waves is 0 and π, respectively. It can be seen from Fig. 5(b) that the electric field is mainly distributed in the short metal strip and the response mode of the absorber to the coherent incident wave is significantly different from the response mode when $\Delta\varphi$ is 0. By comparing Fig. 5(a) and 5(b), it observed that the response of the device to the coherent incident wave can also be affected by phase difference between the incident waves. The total absorption rate of the structure can be modulated at 15.25 THz (the resonant frequency when the phase difference between the coherent incident waves is π).

It can be seen from Fig. 5(c) that the electric field at the 17.75 THz is mainly distributed on both sides of the long metal strip when $\Delta\varphi$ is 0, and proved the long metal strip responds to the frequency of 17.75 THz. At this time, the interaction between the coherent incident wave and the device is strong, and most of the energy carried by the incident wave is converted into electrical and thermal energy, resulting in the total absorption rate of the absorber being close to 1. Fig. 5(d) shows the electric field intensity distribution when the phase difference between the coherent incident waves $\Delta\varphi$ is π at 17.75 THz. It can be found that the electric field strength of the metal strip is much weaker than it shown in Fig. 5(c). The interaction between the coherent incident wave and the device is low and only a small amount of energy carried by the incident wave is consumed which shows that the metasurface is transparent. It indicates that the interaction between the coherent incident wave and the absorber can be changed by adjusting the phase difference between the two incident waves.

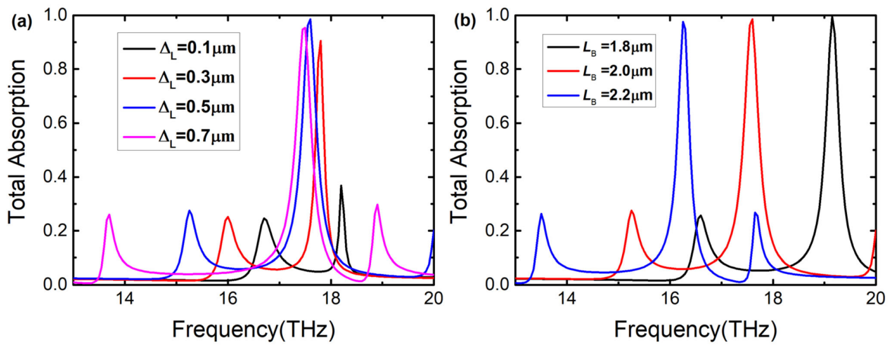

Fig. 6. (a) The relationship between the performance of the coherent controller and the length difference ΔL of different metal strips; (b) the relationship between the performance of the coherent controller and the short metal strip length L_A.

From Fig. 5(a)–5(d), we can indicate that the asymmetry in the structure allows the device to simultaneously modulate the absorption rate of the coherent incident waves at two different frequencies in the working frequency band. The difference between the length of the two different metal strips leads to different response modes and the different resonance peaks appear under different phase differences. The change of the phase difference directly causes the splitting of the resonance frequency. This allows the total absorption rate of coherent incident waves to be adjusted directly by varying the phase difference at resonant frequency.

To optimize the coherent performance of the device, we investigate and optimize the geometric parameters of the structure take the case of $\Delta\varphi$ is 0. First, we investigate the impact of the difference between the long and short metal strips length on the phase-modulating function of the absorption rate. In the simulation, we fixed the short metal strip length L_B and change two metal strips length difference $\Delta_L = L_A - L_B$ by adjusting the long metal strip L_A. In this way, the ΔL is gradually increased from 0.1 μm to 0.7 μm in step of 0.2 μm. The absorption rate under difference Δ_L is obtained and shown in Fig. 6(a). It can be clearly seen that the peak absorption rate is greatly affected while the resonance peak is blue-shifted with the increase of the length difference of the metal strips. When the length between the long and short metal strips is close, the peak absorption of the structure is dramatically decreased, resulting in a rapid decline in the performance of the device. In addition, the peak absorption rate of the absorber will be also greatly affected when the length difference between the metal strips is too large. When the length difference ΔL between the two metal strips is between 0.3μmand 0.5μm, the structure is capable of maintaining a high peak absorption rate.

Then, we investigate the impact of the difference between the long and short metal strips length on the phase-modulating function of the absorption rate. In the simulation, we fixed the short metal strip length L_B and change two metal strips length difference ΔL by adjusting the long metal strip L_A. In this way, the ΔL is gradually increased from 0.1 μm to 0.7 μm in step of 0.2 μm. The absorption rate under difference ΔL is obtained which is shown in Fig. 7(a). It can be clearly seen that the peak absorption rate is greatly affected while the resonance peak is blue-shifted with the increase of the length difference of the metal strips. When the length between the long and short metal strips is close, the peak absorption of the structure is dramatically decreased, resulting in a rapid decline in the performance of the device. In addition, the peak absorption rate of the absorber will be also greatly affected when the length difference between the metal strips is too large. When the length difference ΔL between the two metal strips is between 0.3 μm and 0.5 μm, the structure is capable of maintaining a high peak absorption rate.

Fig. 6(b) shows the results of the total absorption rate of the absorber when the short metal strip length L_A is gradually adjusted from 1.8 μm to 2.2 μm in a step of 0.2 μm with the Δ_L is fixed to 0.5 μm. As can be seen from Fig. 6(b), the change of the length of the metal strip has a greater influence on the peak of the total absorption and when L_A is 2.0 μm, the absorption peak of the coherent control device reaches the highest value of 98.55%. Based on the simulation and analysis,

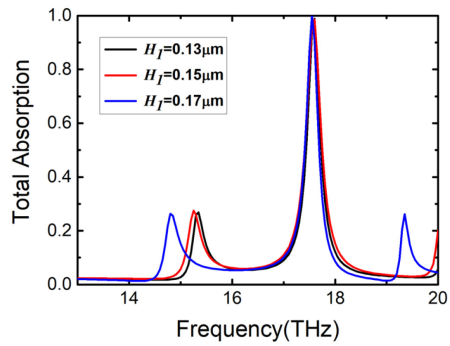

Fig. 7. Schematic diagram of the relationship between coherent controller performance and the thickness of gain material layer H_1.

the device achieves its best performance in terms of peak absorption rate, modulation depth and switching ratio when the thickness of the dielectric layer is set to 0.15 μm and the length of the long and short metal strips is set to 2.0 μm and 2.5 μm, respectively. By adjusting the phase difference between the incident waves and using these geometric parameters, the total absorption of the proposed device to the incident coherent waves can be scanned in the range of 98.55% to 4.21%.

To study the influence of the gain medium layer thickness H_1 on the proposed absorber's performance, other parameters are fixed, and the gain medium layer thickness H_1 is adjusted from 0.13 μm to 0.17 μm in steps of 0.02 μm. The total absorption rates of it under different thickness of the dielectric layer are solved. It can be seen from Fig. 7 that the change of the thickness of the dielectric layer has little effect on the resonance frequency, but has influence on the peak of the total absorption rate. Results also show that when H_1 is 0.15 μm, the absorption peak of the coherent control device reaches the highest value. This due to the lengths of two metal strip respond to two different frequency points. The response frequencies do not shift when the metal strip length does not change, it only changes its total absorption rate.

Based on the simulation and analysis, the device achieves its best performance in terms of peak absorption rate, modulation depth and switching ratio when the thickness of the dielectric layer is set to 0.15 μm and the length of the long and short metal strips is set to 2.0 μm and 2.5 μm, respectively. By adjusting the phase difference between the incident waves and using these geometric parameters, the total absorption of the proposed device can achieve coherent perfect absorption at the frequency of 15.25 THz and 17.75 THz and changing between 27.41% and 98.55%, 27.55% and 97.88%, respectively. In our experiment, the modulation depth of our proposed device is about 5.6 dB and the modulation bandwidth is 0.296 THz. Compared with EAM, this modulation provides a new mechanism and a larger bandwidth compare to EAM which provide a new idea for absorption modulation.

5. Conclusion

A method for controlling the absorption rate of strong waves with weak waves is proposed and a coherent light switch based on metasurface with gain material is proposed in this paper. According to the electric field distribution on the metasurface when the coherent wave is incident under different phase differences, the generation mechanism of the CPA phenomenon and the mechanism of the perfect coherent control device are investigated and analyzed. Results show that the absorption rate can be flexibly regulated by changing the phase difference of the weak control waves and the strong signal waves, the modulation depth of our proposed device is 5.6 dB and the modulation bandwidth is about 0.296 THz. By adjusting the phase difference between the incident waves, the proposed device can obtain the total absorption rate of the incident coherent wave in the range from 27.41% to 98.55% at the frequency of 15.25 THz, and 27.55% to 97.88% at the frequency of 17.75 THz which provide a new idea for absorption modulation. Our finding can contribute to the development of the applications of optical controlled metamaterials such as all-optical switch, modulator and detector in the future.

Acknowledgment

The authors thank the National Key Research and Development Program of China (2019YFB2203903), the National Natural Science Foundations of China (61965006, 61975038, 6194005, 61640409), the Natural Science Foundation of Guangxi Province (2017GXNS-FAA198048, 2018GXNSFAA294099, 2019GXNSFBA245057), Guangxi Project (AD18281092) and the foundation from Guangxi Key Laboratory of Automatic Detecting Technology and Instruments (YQ20107) for their support.

References

[1] S. Takahashi, “Fibers for optical communications,” *Adv. Mater.*, vol. 5, no. 3, pp. 187–191, 1993.
[2] G. B. Huang, Q. Y. Zhu, and C. K. Siew, “Extreme learning machine: Theory and applications,” *Neurocomputing*, vol. 70, no. 1-3, pp. 489–501, 2006.
[3] A. Mokhtar and M. Azizoglu, “Adaptive wavelength routing in all-optical networks,” *IEEE/ACM Trans. Netw.*, vol. 6, no. 2, pp. 197–206, Apr. 1998.
[4] A. R. Mcgurn, “Nonlinear optical media in photonic crystal waveguides: Intrinsic localized modes and deviceapplications,” *Complexity*, vol. 12, no. 5, pp. 18–32, 2010.
[5] A. Luis, “Complementary huygens principle for geometrical and nongeometrical optics,” *Eur. J. Phys.*, vol. 28, no. 2, pp. 231–240, 2007.
[6] K. A. Peacock, “A possible explanation of the superposition principle,” *Physics*, 2002. [Online]. Available: http://arxiv.org/abs/quant-ph/0209082v1
[7] A. Sinha, A. H. Vijay, and U. Sinha, “On the superposition principle in interference experiments,” *Sci. Rep*, vol. 5, 2015, Art. no. 10304.
[8] S. A. Mousavi, E. Plum, J. Shi, and N. I. Zheludev, “Coherent control of birefringence and optical activity,” *Appl.Phys. Lett.*, vol. 105, 2014, Art. no. 067402.
[9] J. Shi, X. Fang, E. T. F. Rogers, E. Plum, K. F. MacDonald, and N. I. Zheludev, “Coherent control of snell’s law at metasurfaces,” *Opt. Exp.*, vol. 22, no. 17, pp. 21051–21060, 2014.
[10] X. Fang, K. F. MacDonald, and N. I. Zheludev, “Controlling light with light using coherent metadevices: All-optical transistor, summator and invertor,” *Light. Sci. Appl.*, vol. 4, no. 5, 2014, Art. no. e292.
[11] J. Zhang, K. F. Macdonald, and N. I. Zheludev, “Controlling light-with-light without nonlinearity,” *Light. Sci. Appl.*, vol. 1, no. 7, 2012, Art. no. e18.
[12] M. Papaioannou, E. Plum, E. T. Rogers, and N. I. Zheludev, “All-optical dynamic focusing of light via coherent absorption in a plasmonic metasurface,” *Light. Sci. Appl.*, vol. 7, no. 3, 2018, Art. no. 17157.
[13] X. Fang, M. Lun Tseng, J.-Y. Ou, K. F. MacDonald, D. Ping Tsai, and N. I. Zheludev, “Ultrafast all-optical switching via coherent modulation of metamaterial absorption,” *Appl. Phys. Lett.*, vol. 104, no. 14, 2014, Art. no. 141102.
[14] Y. Ye, D. Hay, and Z. Shi, “Coherent perfect absorption in chiral metamaterials,” *Opt. Lett.*, vol. 41, no. 14, pp. 3359–3362, 2016.
[15] X. Zhang and Y. Wu, “Scheme for achieving coherent perfect absorption by anisotropic metamaterials,” *Opt. Exp.*, vol. 25, no. 5, pp. 4860–4874, 2017.
[16] D. Xiao, K. Tao, Q. Wang, Y. Ai, and Z. Ouyang, “Metasurface for multiwavelength coherent perfect absorption,” *IEEE Photon. J.*, vol. 9, no. 1, pp. 1–8, Feb. 2017.
[17] H. J. Chen, C. Z. Chen, X. W. Fang, Y. Li, and X.-D. Tang, “Controllable coherent perfect absorption and transmission in a generalized three-mode optomechanical system,” *Optik*, vol. 168, pp. 46–53, 2018.
[18] X. B. Yan, C.-L. Cui, K.-H. Gu, X.-D. Tian, C.-B. Fu, and J.-H. Wu, “Coherent perfect absorption, transmission, and synthesis in a double-cavity optomechanical system,” *Opt. Exp.*, vol. 22, no. 5, pp. 4886–4895, 2014.
[19] W. Zhu, F. Xiao, K. Ming, and M. Premaratne, “Coherent perfect absorption in an all-dielectric metasurface,” *Appl. Phys. Lett.*, vol. 108, no. 12, 2016, Art. no. 121901.
[20] Z. Li *et al.*, “Full-space cloud of random points with a scrambling metasurface,” *Light. Sci. Appl.*, vol. 7, no. 1, pp. 63–70, 2018.
[21] J. Deng *et al.*, “Spatial frequency multiplexed meta-holography and meta-nanoprinting,” *ACS Nano*, vol. 13, no. 8, pp. 9237–9246, 2019.
[22] S. Sandhu, M. L. Povinelli, and S. Fan, “Enhancing optical switching with coherent control,” *Appl. Phys. Lett.*, vol. 96, no. 23, pp. 231108–231108–3, 2010.
[23] T. G. Mayerhofer, H. Mutschke, and J. Popp, “The electric field standing wave effect in infrared transmission spectroscopy,” *Chemphyschem.*, vol. 18, no. 20, pp. 2916–2923, 2017.
[24] C. Yan *et al.*, “Coherent perfect absorption of electromagnetic wave in subwavelength structures,” *Opt. Laser Technol.*, vol. 101, pp. 499–506, 2018.
[25] L. Baldacci, S. Zanotto, G. Biasiol, L. Sorba, and A. Tredicucci, “Interferometric control of absorption in thin plasmonic metamaterials: general two port theory and broadband operation,” *Opt. Express*, vol. 23, no. 7, pp. 9202–9210, 2015.
[26] S. Zanotto, F. Bianco, and V. Miseikis, “Coherent perfect absorption and transparency in lossy and loss/gain metasurface-embedding structures,” in *Proc. IEEE Int. Conf. Transparent Opt. Netw.*, 2017.